Annular Groove Phase Mask: an achromatic vortex coronagraph for differential polarimetric imaging

Dimitri Mawet[1], and the SEE-COAST team

[1] *Institut d'Astrophysique et de Géophysique, Université de Liège, Belgium*

E-mail : mawet@astro.ulg.ac.be

Introduction

Speckle subtraction/calibration techniques such as Spectral Differential Imaging (or SDI) and Polarimetric Differential Imaging (PDI) have been opposed to coronagraphy for a long time. It is only recently that second generation XAO instruments have brought both concepts to work together but always in cascade or separately (e.g. GPI and SPHERE). We propose to combine the three instrumental approaches in a single one: a coronagraphic spectro-polarimeter. With a classical Lyot amplitude coronagraph, the spectro-polarimeter can be considered independently and implemented downstream the coronagraph (like on GPI). With a phase-mask coronagraph, which intrinsically allows accessing much smaller IWA, this is not possible due to the polarization properties of the coronagraph. It must therefore be implemented inside the spectro-polarimeter. If this implementation is conducted wisely, each subsystem can take advantage of the other, as we will demonstrate here below. The key point is that the number of spectral channels can seriously be reduced without sacrificing the performances. Indeed, the implementation of a particular coronagraph (AGPM) in the polarization-filtered system provides a significant gain in rejection allowing an "ultimate" achromatization. The Annular Groove Phase Mask (AGPM) is a broadband vectorial vortex coronagraph consisting of integrated subwavelength optical elements. In this poster, we will show why the polarization properties of the AGPM are well suited to differential polarimetric imaging. Using this special ability, we will present an instrumental concept of imaging coronagraphic spectro-polarimeter for the 1.5-meter Super Earth Explorer-Coronagraphic Off-Axis Space Telescope (SEE-COAST). Preliminary performance assessment in presence of realistic sources of noise (wavefront errors, non-common path aberrations, mask and optical component imperfections, etc.) leads to 10^{-9} contrasts after speckle subtraction, over a 50 %-bandwidth in the visible wavelength range and at inner working distances as small as 1 λ/d. The AGPM is basically a vortex of topological charge lp=2, leading to a θ^2 sensitivity to tip-tilt. Thanks to optical integration, we will show how to practically increase the topological charge and therefore decrease the tip-tilt sensitivity, which can be useful especially for larger telescopes

Annular Groove Phase Mask Coronagraph

The Annular Groove Phase Mask (AGPM) is the natural evolution of the well-proven **Four Quadrant Phase Mask coronagraph** (Rouan *et al.* 2000). The initial purpose of the AGPM coronagraph was to suppress the "dead zones" resulting for the quadrant transitions of the FQPM. The AGPM (see Mawet *et al.* 2005) coronagraph consists of a space-variant subwavelength grating (Fig. 1) synthesizing a so-called **vectorial optical vortex** of topological charge lp=2, analytically leading to a total starlight rejection in the theoretically perfect case (perfect component, no WFE, unobscured pupil, perfect centering of the star on the optical axis,...). It is to be emphasized that the AGPM nominally works in unpolarized natural light.

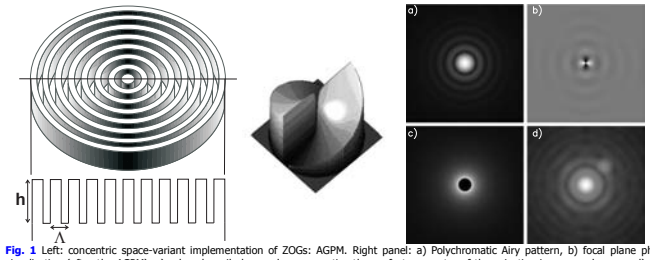

Fig. 1 Left: concentric space-variant implementation of ZOGs: AGPM. Right panel: a) Polychromatic Airy pattern, b) focal plane phase visualisation (after the AGPM), c) relayed pupil plane, where we notice the perfect symmetry of the rejection in an annular way, d) final coronagraphic image revealing the 15 mag fainter simulated companion. All images are displayed in non linear scale.

In the real world however, nothing is perfect. **Subwavelength gratings** are known to **synthesize artificial birefringent elements** but they certainly are not perfect vectorial phase shifters and induce differential losses which can be quantified by **rigorous diffraction analysis** leading to a thorough description of the component by the following Jones matrix in the helical (circular polarization) basis (*):

$$AGPM = \frac{1}{2}\left(\eta_{TE} + \eta_{TM} e^{i\Delta\phi}\right)\begin{bmatrix} 1 & 0 \\ 0 & 1 \end{bmatrix} + \frac{1}{2}\left(\eta_{TE} - \eta_{TM} e^{i\Delta\phi}\right)\begin{bmatrix} 0 & e^{i2\theta} \\ e^{-i2\theta} & 0 \end{bmatrix}$$

Where η_{TE} and η_{TM} are the subwavelength grating diffraction efficiencies in the zeroth order for the orthogonal polarizations TE (transverse electric, or s) and TM (transverse magnetic, or p) and $\Delta\phi$, the phase shift (retardance) between them. Ideally, $\eta_{TE} = \eta_{TM} = 1$ and $\Delta\phi = n$ whatever the wavelength (achromaticity Holy Grail) so that the incoming circular polarization is reversed (left-handed becomes right-handed and vice-versa) and affected by a pure optical vortex $e^{\pm i2\theta}$, leading to a perfect attenuation of the on-axis coherent starlight. In practice, the inevitable departure from this nominal case is proportional to the working bandwidth. Then, a residual of weight $\frac{1}{2}(\eta_{TE}+\eta_{TM}e^{i\Delta\phi})$ appears and contaminates the pure vortex. **The key point is that this residual, bearing all the component imperfections has the same polarization state as the incoming one, where the vortex has been transferred in the reverse polarization**. Therefore, appropriate filtering at the input and the output of the component should remove these imperfections and lead to improved performances with respect to the natural unpolarized light case.

(*) in the circular (helical) polarization basis, the unitary polarization vectors are either the right-handed one [1 0] or the left-handed one [0 1]. The helical-basis transformation matrix U that allows switching between the classical linear and helical basis is defined by => $U = \frac{1}{\sqrt{2}}\begin{bmatrix} 1 & i \\ 1 & -i \end{bmatrix}$

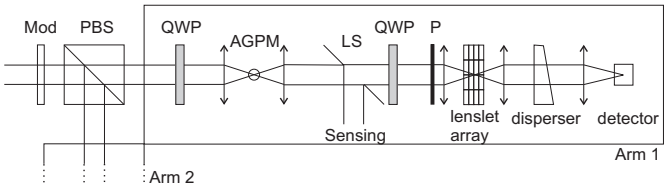

Fig. 2 Preliminary optical schematic of the AGPM-differential polarimetric spectro-imager instrumental concept in the frame of the SEE-COAST project. The beam is first slowly modulated by a variable retarder (LCVR, FLC or PEM, or simply a rotating halfwave plate), then split by a polarizing beamsplitter (PBS) into two equivalent arms of orthogonal linear polarizations (Arm 1 and 2). QWP are achromatic quarterwave plates that convert the linear polarization to the circular one to efficiently feed the AGPM coronagraph. LS stands for Lyot stop, which is a diaphragm reflecting the residual starlight to a sensing unit (star fine centering on the coronagraph). The IFS is based on a TIGER-type lenslet-array.

This polarization property of the AGPM makes it a coronagraph especially suited to differential polarimetric imaging provided that it is properly implemented inside the polarimeter. Its symmetry also allows for alternate switching between two orthogonal polarization states that are linear at the input. In conclusion, a polarimetric system which converts the polarization signal with a polarization modulator into a temporal intensity modulation can be designed to accommodate the AGPM coronagraph (Fig. 2), leading to a **symbiosis** (both concepts can take advantage of the other) and substantial performance improvements. One key point is that in space, the polarimetric modulation can be much slower than for ground-based polarimeters such as ZIMPOL (Schmid *et al.* 2006). Theoretical analysis using Jones formalism allows us to calculate the attenuation gain provided by the polarization filtering (Table 1). The conclusion is that the limitation does not come from the coronagraph anymore but from the polarization optics.

Table 1. Theoretical results in terms of total attenuation and contrast of the AGPM with polarization filtering, neglecting WFE issues and therefore speckle subtraction/calibration.

AGPM natural light broadband rejection (R~2)	Polarizer ER	QWP accuracy	Total attenuation integrated over the whole discovery space	Broadband contrast at 1.5 λ/d
500-1000	**10^4**	**0.5 rad PTV**	**5 x 10^{-5}**	**~ 10^{-6}**
500-1000	**10^4**	**0.1 rad PTV**	**5 x 10^{-7}**	**~ 10^{-8}**
500-1000	**10^6**	**0.1 rad PTV**	**5 x 10^{-8}**	**~ 10^{-9}**

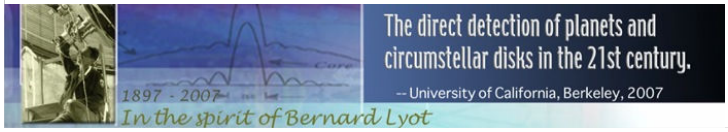

Error sources

We have already taken into account polarization element errors, i.e. finite extinction ratio for polarizers and retardance errors for waveplates. Ghost problems, mostly due to the polarization components before the coronagraph are also to be minimized. Classical solutions are state-of-the-art antireflective treatments and proper implementation of the components. For instance, we could use the "wedging" method which has been developed in infrared nulling interferometry for the same purpose. The stray light dumping should not degrade polarization and should not introduce too much spectral and polarization dispersions. It must stay in the 1 mas centering range (a slight dispersion will be considered in the numerical simulation presented below).

WFE upstream the coronagraphs, resulting from the telescope optical assembly, relay optics and polarization components, are **critical** and will necessitate **active and/or passive correction** systems. However, the philosophy of the SEE-COAST project is to trade-off the requirements on the optical surface quality with the active correction subsystems complexity. The idea is to request a WFE of $\lambda/100$ rms before the coronagraph to allow it to provide a rough attenuation of 10^{-5}-10^{-7}. Then, speckle-calibration techniques such as PDI and SDI will help reaching the final 10^{-9} contrast goal, provided that non-common path errors between the calibration channels do not exceed ~1 nm rms.

Numerical simulations

Hypothesis:

-No ghosts

-Common path errors/aberrations:

Input DSP= $f^{-1.5}$
Input WFE = λ/100 rms (λ=632.8nm)
Bandwidth = 450-800 (10 points)
Coronagraph = AGPM (SiO_2) with a natural (unpolarized) rejection performance of ~ 500
Phase errors (λ)
Amplitude errors (λ)
Polarizer: ER=10^4 (commercially available)
Waveplate: achromatic quarterwave plate (n ± 0.1 rad)
Phase errors (λ)
Output DSP= $f^{-1.5}$
Output WFE = λ/100 rms (λ=632.8nm)

-Non-common path errors/aberrations:

Before the coronagraph:
Chromatic dispersion 2 mas between 450 and 800 nm.
Polarization differential dispersion between s and p: 0.5 mas.

After the coronagraph:
Crossed (90°) dispersion
Non-common path errors DSP = $f^{-1.5}$
WFE = λ/1000 rms (0.6 nm rms).

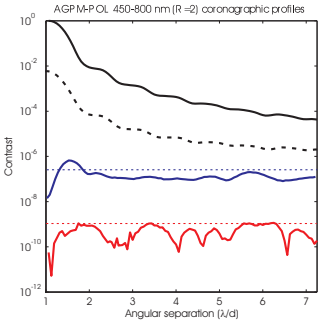

Fig. 3 Coronagraphic profiles generated by a numerical simulation taking into account the hypothesis mentioned in the left panel. The code is a traditional Fourier coronagraphic code. The coronagraph modelization is complex and involve a rigorous diffraction analysis interfaced to the coronagraphic code thanks to the Jones formalism. Black curve: polychromatic Airy profile (450-800 nm). Black dotted curve: AGPM coronagraphic profile in unpolarized broadband (50%-bandwidth) light. Blue curve: the same after polarization filtering. Red curve: contrast after polarimetric speckle subtraction/calibration.

Note about sensitivity to tip-tilt and stellar diameter

Sensitivity to tip-tilt and stellar diameter of the AGPM basically grows as θ^2. Given the small diameter of SEE-COAST (1.5 meters) and the baseline WFE of $\lambda/100$ rms, this seems a priori sufficient to reach the 10^{-6}-10^{-7} rough attenuation floor before speckle subtraction (Fig. 3). Speckle calibration thanks to differential imaging should remove the starlight residual, be it resolved or not. However, temporal variations due to jitter for instance may anyway require to increase the power of the sensitivity to this low-order aberration. For that, we must **increase the topological charge of the vortex** because the dependency θ^n to the aberration directly scale with it, n=lp (see Mawet *et al.* 2005). Two solutions exist. The first one is to implement the space-variant grating in another pattern intrinsically generating a higher topological charge (see Fig. 4, left). The second one is original, and allows keeping the AGPM geometry which is more convenient to manufacture. The principle is to stack two AGPM with a halfwave plate (represented by the Jones matrix [0,-i;-i,0] in the helical basis) between them (unlike scalar vortices, the topological charges of vectorial vortices do not simply add). Doing so, the AGPM topological charge is easily incremented from lp=2 to lp=4:

$$\begin{bmatrix} 0 & e^{i2\theta} \\ e^{-i2\theta} & 0 \end{bmatrix}\begin{bmatrix} 0 & -i \\ -i & 0 \end{bmatrix}\begin{bmatrix} 0 & e^{i2\theta} \\ e^{-i2\theta} & 0 \end{bmatrix} = -i\begin{bmatrix} 0 & e^{i4\theta} \\ e^{-i4\theta} & 0 \end{bmatrix}$$

This can be iterated to provide any even topological charge and thus sensitivity to low-order aberration. Note that the stack can be integrated in a few microns on top of a substrate thanks to the subwavelength grating technology.

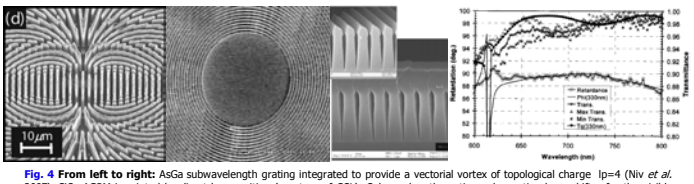

Fig. 4 From left to right: AsGa subwavelength grating integrated to provide a vectorial vortex of topological charge lp=4 (Niv *et al.* 2007). SiO_2 AGPM imprinted by direct laser writing (courtesy of CSL). Subwavelength grating achromatic phase shifter for the visible wavelength range with spectral characterization (Deng et al. 2005, NanoOpto).

Conclusion: prototyping

Vectorial vortices up to topological charges of 4 (Fig. 4, left) based on subwavelength optical elements are extensively studied by Erez Hasman's group at Israel Institute of Technology, mainly for CO_2 laser applications (Niv *et al.* 2007). Their micro-components are manufactured with *AsGa* substrates. As far as the AGPM is concerned, H/K-band prototype manufacturing is about to begin at CEA-LETI in the framework of VLT's SPHERE R&D activities, we should test them this year. Silicon micro-structuring technologies inherited from micro-electronics will be used. The "Centre Spatial de Liège" has also begun prototype manufacturing (Fig. 4) on SiO_2 samples, also for the near-infrared. Making subwavelength gratings for the visible wavelength range is not trivial. The period of the grating must absolutely be smaller than λ/n, n being the index of refraction of the chosen substrate material. We therefore have to deal with periods in the 300 to 400 nm range according to the material. Controlling the micro-structure at such scales is challenging but feasible using for instance nano-imprint lithography techniques. In this context, let us cite the work of Deng *et al.* (2005) for optical pickup units. They indeed proposed, manufactured and tested (now commercialize) achromatic subwavelength grating waveplates for the visible. Converting the performance of their manufactured components (Fig. 4, left) in terms of nulling efficiency would lead to a 1000 rejection ratio over a bandwidth of more than 20 % in natural light which is sufficient for the proposed concept. There is still room for improvement. NanoOpto has been contacted to make AGPM prototypes.